Contract No.:

This manuscript has been authored by Savannah River Nuclear Solutions (SRNS), LLC under Contract No. DE-AC09-08SR22470 with the U.S. Department of Energy (DOE) Office of Environmental Management (EM).

Disclaimer:

Matrix Assisted Ionization of Molecular Uranium Species

Danielle R. Mannion, Joseph M. Mannion, Wendy W. Kuhne, Matthew S. Wellons*

Savannah River National Laboratory, Aiken, South Carolina 29803

ABSTRACT: Matrix-assisted ionization (MAI) demonstrates high sensitivity for a variety of organic compounds; however, few studies have reported the application of MAI for the detection and characterization of inorganic analytes. Trace-level uranium analysis is important in the realms of nuclear forensics, nuclear safeguards, and environmental monitoring. Traditional mass spectrometry methods employed in these fields require combinations of extensive laboratory chemistry sample preparation and destructive ionization methods. There has been recent interest in exploring ambient mass spectrometry methods that enable timely sample analysis and higher sensitivity than what is attainable by field-portable radiation detectors. Rapid characterization of uranium at nanogram levels is demonstrated in this study using MAI techniques. Mass spectra were collected on an atmospheric pressure mass spectrometer for solutions of uranyl nitrate, uranyl chloride, uranyl acetate, and uranyl oxalate utilizing 3-nibrobenzonitrile as the ionization matrix. The uranyl complexes investigated were detectable, and the chemical speciation was preserved. Sample analysis was accomplished in a matter of seconds, and limits of detection of 5 ng of uranyl nitrate, 10 ng of uranyl oxalate, 100 ng of uranyl chloride, and 200 ng of uranyl acetate were achieved. The observed gas-phase speciation was similar to negative-ion electrospray ionization of uranyl compounds with notable differences. Six matrix-derived ions were detected in all negative-ion mass spectra, and some of these ions formed adducts with the uranyl analyte. Subsequent analysis of the matrix suggests that these molecules are not matrix contaminants and are instead created during the ionization process.

INTRODUCTION

Characterization and detection of trace quantities of uranium is an important diagnostic and analytical metric for a variety of nuclear fuel cycle monitoring activities including environmental monitoring[1-2], nuclear forensics[3-5], and nuclear safeguards[6-10]. Mass spectrometry (MS) based techniques are the gold standard for uranium isotope ratio measurements (i.e., thermal ionization, inductively coupled plasma, and accelerator MS) as these methods simultaneously provides low level detection (i.e. sub-picograms) and accurate isotopic composition information. Traditional MS based uranium isotope analyses often require extensive, time-consuming, and expensive wet-chemistry for sample preparation[11]. Recent efforts have focused on developing ambient MS methods for uranium analysis. These methods offer the advantages of rapid analysis, soft ionization, and the potential to minimize current MS sample process requirements and instrumentation overhead burdens. Electrospray ionization (ESI) MS, a type of ambient MS, has been used since the 1990s to analyze inorganic compounds in solution[12-17], including uranium species[18-28]. ESI has been used extensively to investigate the coordination chemistry of uranyl ligand complexes in the gas phase via collision induced dissociation (CID)[17, 19-25, 27], ion-molecule reactions[20-22, 27], and spectroscopic techniques[20, 29-30]. More recently, paper spray ionization (PSI) MS has been employed to analyze inorganic species[31-32], including uranyl complexes[33]. By virtue of soft ionization, these ambient MS methods can generate uranyl ion species with intact ligands and potentially allow for identification of the progenitor chemical composition prior to dissolution[34-36].

Ambient MS methods based on matrix-assisted ionization (MAI) have not seen any exploratory effort for uranium species detection and analysis, though there has been extensive research on organic analysis in the brief time since its discovery[37-50]. The advantages of MAI-MS are the elimination of high voltage, a heat source, lasers, and/or compressed gases in the ionization process and minimal sample preparation requirements[51]. Due to the ease of sample preparation, no direct ionization energy requirements, and lack of compressed gasses, MAI has shown promise as a field-portable method for biological and synthetic materials[52]. Development of MAI-MS techniques may bridge the technology gap between traditional high-sensitivity laboratory MS techniques and field-portable radiation detectors enabling rapid on-site analyses with minimal sample preparation and improved detection limits over counting techniques for long-lived species such as uranium. The reported effort focuses on exploring MAI for the detection and characterization of simple uranyl complexes with 3-nitrobenzonitrile (3-NBN) as the ion generating matrix and is the first demonstration of direct MAI uranium detection and characterization.

Numerous organic compounds have demonstrated MAI behavior but 3-NBN is the ubiquitous ionization matrix material commonly utilized in the prior published efforts[39, 41-43, 46, 48-49, 52-53]. With this preponderance of 3-NBN centric MAI research and because this matrix does not require a heated MS inlet it was selected for this study. Analytes explored were uranyl hydrate complexes of nitrate, chloride, acetate, or oxalate speciation. Ionized forms of these species were putatively identified for all

four species as uranyl associated with various combinations of ligands and/or other conjugate anions. No method optimization was attempted, and <200 ng limits of detection was achieved for all species. In all negative-ion MAI experiments six discrete ions with >10% relative ion intensity and at mass range <275 m/z were detected. These ions were present in the mass spectra both with and without uranium-bearing analytes present. Although these ion species are not unambiguously identified, the current hypothesis is the 3-NBN MAI processes within these experiments generate the organic anions from the matrix itself. Attempts to determine if the organic anions were 3-NBN chemical impurities by complementary high-resolution methods were negative.

EXPERIMENTAL

Samples were analyzed with a time-of-flight AccuTOF DART 4G mass spectrometer (JEOL, Peabody, MS, USA). High precision mass measurements were obtained by performing a DART calibration with Fomblin Y (HVAC 16/6, Sigma-Aldrich, St. Louise, MO) at the end of a sample analysis series. Select analyses of reagents were performed on a high-resolution 7250 GC/Q-TOF (Agilent Technologies, Santa Clara, CA). Instrument operation parameters are detailed in the Supporting Information. Stock solutions of uranyl chloride, uranyl acetate, and uranyl oxalate salts composed of natural uranium (International Bio-Analytical Industries, Boca Raton, FL) were used to make solutions of 1, 10, 50, 100, 250, and 500 µg/mL of each uranyl salt in ASTM Type II water. A stock solution of depleted uranium certified reference material U005 (New Brunswick Laboratory, Argonne, IL) was used to make solutions of 0.1, 0.5, 1, 10, 50, and 100 µg/mL uranyl nitrate in 2% nitric acid. Samples were prepared for MAI analysis by mixing each sample with methanol (ACS Reagent Grade, Sigma-Aldrich, St. Louis, MO) to create 50:50 sample/methanol mixtures.

Uranyl MAI analysis was first attempted by introducing dried matrix/analyte crystals into the atmospheric pressure orifice; however, the 400 micron orifice diameter precludes reproducible introduction via this method. Sample analysis was instead conducted using a previously reported sample introduction technique where similar instrumentation was used[46]. This technique involves aspirating liquid sample saturated with suspended matrix crystals into the mass analyzer via the atmospheric pressure orifice. Immediately prior to analysis, approximately 5–10 mg of 3-NBN (98% purity, Sigma-Aldrich, St. Louis, MO) was added to each uranyl sample, enough to fill approximately half the liquid sample with undissolved crystals. The vials were shaken by hand to homogenize the matrix crystals in solution immediately prior to subsampling. A disposable glass capillary (5 µL, DWK Life Sciences, Millville, NJ) was dipped into the sample, and 1–5 µL of sample with matrix crystals was drawn into the tube through capillary action. This aliquot was aspirated directly into the mass spectrometer sample orifice, with 10 aspirations performed for each sample concentration (Figure S1). This sample introduction technique greatly diminished the occurrence of orifice matrix induced obstruction but led to memory effects. To minimize the impact of carryover on uranyl ligand analysis, the sample cones and ring lens were cleaned after each sample series. A reagent blank consisting of 3-NBN/water/methanol or 3-NBN/2% nitric acid/methanol was analyzed at the beginning and end of each sample series (Figure S2).

RESULTS AND DISCUSSION

The uranyl ligands analyzed were only detected in negative-ion mode and when aspirating liquid sample saturated with suspended 3-NBN crystals. All spectra contained uranyl ion species with some combination of two species labeled M1 and M2 based on reproducible putative mass identification but of unknown chemistry. We hypothesize M1 and M2 are matrix-derived species, and this explanation is detailed in the subsequent discussion. A complete identification of all detected uranyl ion complexes is described in the Supporting Information (Table S1). Similar analyses were attempted in positive-ion mode, but no ions corresponding to potential uranyl-containing analytes were observed. Spectra generated in positive-ion mode from 3-NBN reagent blanks and uranyl ligands were dominated by a potential matrix peak at m/z 434; no other peaks could be identified as uranium-bearing ions (Figure S3). Methanol solutions of uranyl species without 3-NBN were tested in positive- and negative ion-modes but no ion signal above background was detected. This lack of ion generation without the presence of 3-NBN is consistent with MAI processes being responsible for ion formation instead of other mechanisms such as solvent-assisted ionization (SAI).

The four uranyl ligand species examined were all detected as negative-ion complexes composed of one uranyl cation in conjugation with anions totaling three negative charge equivalents. For all species, uranium was in a 6+ oxidation state based on simple charge balance of the total ion. Uranyl nitrate was primarily observed as uranyl complexed with three nitrates $[(UO_2)(NO_3)_3]^-$, although other ion complexes were observed that correspond to the oxo-nitrate $[(UO_2)(NO_3)_2(O)]^-$ and hydroxy-nitrate $[(UO_2)(NO_3)(OH)_2]$ adducts (Figure 1a). The detection of these complexes is similar to what was observed in previously reported negative-ion ESI studies of uranyl compounds[17, 22, 26]. Investigation of the ESI-produced $[(UO_2)(NO_3)_3]^-$ complex by infrared multiple photon photodissociation (IRMPD) demonstrated strong bonding between the nitrates and the metal center.[29] Those authors suggested the high ion intensity of this complex is due to its gas-phase stability and is consistent with relative intensity observed in the MAI mass spectra shown in Figure 1a. The $[UO_2(NO_3)_3]^-$ ion is also known to form in alcohol/water solutions. The analyte solution for the uranyl nitrate MAI experiments contained 2% nitric acid so the trinitrate complex is expected to be present in the solution phase. The $[(UO_2)(NO_3)_2(O)]-$ complex may be the product of fragmentation of the trinitrate complex resulting in the loss of NO_2; this behavior has been observed in CID studies of gas-phase uranyl trinitrate[22, 54]. Unlike commensurate ESI studies of uranyl nitrate analyte, a $[(UO_2)(NO_3)_2(M2)]^-$ ion species is also observed with MAI.

MAI generated uranyl chloride ions were identified as uranyl complexes containing combinations of chloride, M1, and/or M2 (Figure 1b) with stoichiometric formulate of $[UO_2Cl_3]^-$, $[UO_2(Cl)_2(M2)]^-$, $[UO_2(Cl)(M2)(M1)]^-$, and $[UO_2(M2)_2(M1)]^-$ among others (SI, Table S1). No other adducts were observed above the 10% ion intensity threshold. Previous studies utilizing ESI-IMS-TOFMS solely observed generation of the chloride adduct ion $[UO_2Cl_3]^-$.[26] The authors suggested the lack of other ion species was due to chloride's high electron affinity. This contrasts with the MAI-MS spectra generated in this study, where chloride ligands are nominally displaced by M1 and M2 species. This suggests that species M1 and M2 have comparable affinity to uranyl but further study is required to conclusively characterize ligand affinity.

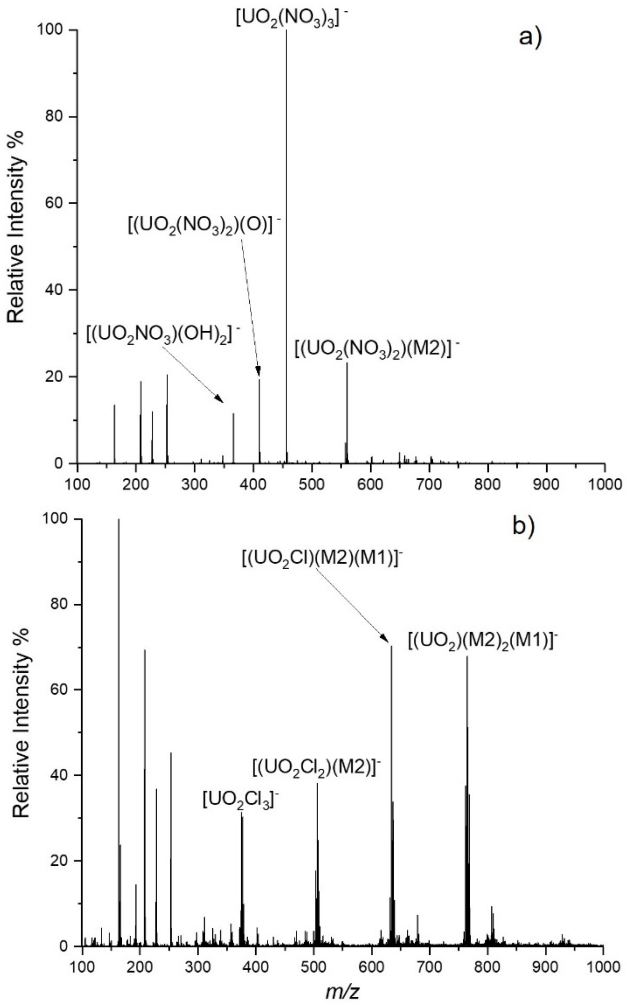

Figure 1. Negative ion MAI mass spectra of uranyl nitrate (a) and uranyl chloride (b) labeled with putative ion complex compositions. Ion intensity peaks < 275 *m/z* are identified in Figure 2.

MAI of uranyl acetate was found to be similar to uranyl nitrate in that the predominate ion generated is uranyl complexed with three acetates $[UO_2(CH_3CO_2)_3]^-$ (SI, Figure S5(a)). The triacetate ion complex and two other ion species characterized as $[UO_2(CH_3CO_2)_2O_2]^-$ and $[UO_2(CH_3CO_2)_2OH]^-$ are similar to those generated by ESI[24, 26-27]. Unlike ESI, ion complexes were identified which include matrix-derived species M1 and M2 such as $[UO_2(CH_3CO_2)_2(M2)]^-$, $[UO_2(CH_3CO_2)(M2)(M1)]^-$, $[UO_2(M2)_2(M1)]^-$, and many others (SI, Table 1). Comparable to other species examined in this study, M1 and M2 adducts were identified in a significant portion of uranyl containing ions. Additionally, the ion complex $[UO_2(M2)_2(M1)]^-$ is identified in MAI generated ions from both uranyl chloride and uranyl acetate.

Uranyl oxalate MAI analysis generated the most complex spectra of the uranyl ligands analyzed within this preliminary study. Oxalate was the only bidentate uranyl ligand tested possessing a 2– charge. Regardless, all uranyl oxalate ions detected maintained the U^{6+} oxidation state with a commensurate reduction in uranyl ligand moieties from three to two when the oxalate ligand was a component of the ion complex (Figure S5(b)). Unique features of the uranyl oxalate spectra include the presence of hydroxide anions in complexes that lack the oxalate ligand, and the detection of uranyl in complex with three hydroxide moieties as $[UO_2(OH)_3]^-$. Note that the uranyl oxalate stock solution contained an excess of oxalic acid to assist solution stability. Further research is required to unambiguously characterize this uranyl-ligand system, and no commensurate ESI efforts could be found in the literature for comparison.

Signal to noise ratios for the highest abundance ion species were used to calculate limit of detection (LOD) for each of the uranyl species analyzed. Integrated peak areas were extracted from the ion chromatograms of the 10 replicate measurements at each concentration. Linear regression plots were made of signal to noise verse concentration, and the linear range was used to create linear regression formulas (see the SI). These were used to calculate a LOD of 5 ng of uranyl nitrate, 10 ng of uranyl oxalate, 100 ng of uranyl chloride, and 200 ng of uranyl acetate. Since the volume of sample was not strictly controlled for each sample aspiration but was visually confirmed to be 5 µL or less, calculations were performed assuming 5 µL of sample introduction and no uranium concentration by the matrix.

All MAI experiments preformed on uranyl analytes in negative-ion mode demonstrated a series of high ion intensity peaks in the mass range <275 m/z and are attributed to 3-NBN matrixed derived ions. The corresponding mass spectra from a 3-NBN/water/methanol test slurry without any uranyl analytes is shown in Figure 2. Six ion species are readily discernable with >10% relative intensity and were labeled M1, M2, ...M6 or M* in aggregate (Table S2). Supplemental measurements of 3-NBN solutions were characterized on the high-resolution Agilent 7250 GC/Q-TOF in order to assess if these species were potential matrix contaminants (Figure S4). No significant molecular ions with any M* m/z were present in all measurements conducted within a 5 ppm error of the experimentally measured M* masses. Multiple measurement iterations were also performed on the JEOL AccuToF to ensure these ions were not the product of laboratory chemical cross contamination or solvent impurities. This absence of chemical impurities suggests M* anions are formed during the MAI process from the 3-NBN matrix and/or from in situ reactions within the mass spectrometer inlet region.

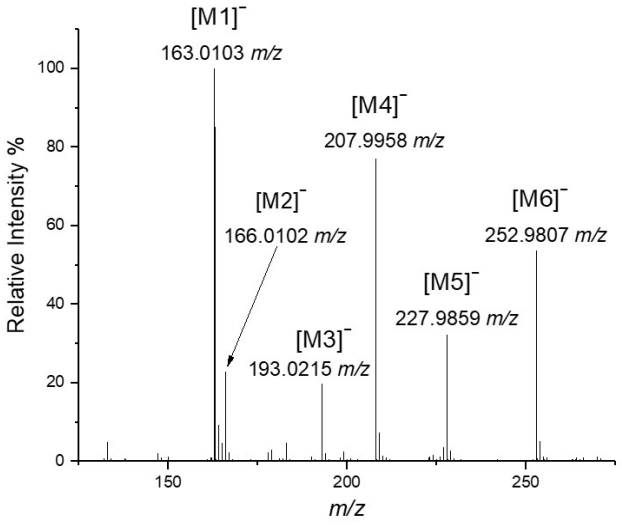

Figure 2. Negative ion mass spectra of 3-NBN matrix in water/methanol showing *m/z* region containing matrix-derived ions with assigned identities and calibrated mass.

As the molecular compositions of M* are not established, all ppm error was calculated using the exact mass of the uranyl complexes and the measured mass of matrix ions. The ppm error formula used is supplied in the SI. Although the chemical

identity of these species was not known, their putative mass values were used to identify M1 and M2 within the various uranyl complexes described herein. Analysis of these matrix ion species utilizing MS/MS, CID, and/or spectroscopic techniques will assist in future putative identification.

Only the matrix-derived anions M1 and M2 were detected as constituents of the uranyl ion complexes as shown in Table 1. M2 was associated with uranyl ion species generated from all four uranyl analytes tested. M1-containing uranyl ion complexes were only generated from uranyl chloride and acetate analytes. Incidentally, uranyl acetate and chloride demonstrated strong ion signals which corresponded to a complete loss of original ligands with ion species identified as $[UO_2(M^*)_3]^-$ where M* is a combination of only M1 and M2. Uranyl oxalate was also detected without the corresponding ligand and in complex with M2 and hydroxide.

Table 1. Select exemplars of uranyl ion complexes containing matrix-derived anions (M1 and M2 m/z assumed as measured).

Proposed Identity	Measured Mass	ppm
Uranyl Nitrate ($UO_2(NO_3)_3$)		
$[UO_2(NO_3)_2$ (M2)$]^-$	560.0247	3.17
Uranyl Chloride (UO_2Cl_2)		
$[UO_2Cl$ (M1) (M2)$]^-$	634.0321	3.35
UO_2Cl_2 (M2)$^-$	505.9865	4.17
Uranyl Acetate ($UO_2(CH_3CO_2)_2$)		
$UO_2(CH_3CO_2)_2$ (M2)$^-$	554.0792	3.06
$UO_2(CH_3CO_2)_2$ (M1)$^-$	551.0784	1.59
Uranyl Oxalate ($UO_2C_2O_4$)		
$UO_2(C_2O_4)$ (M2)$^-$	524.0314	1.63
$UO_2(OH)_2$ (M2)$^-$	470.0571	1.63

Because the uranyl analyte forms several uranyl ion complexes which contain matrix-derived anions M1 and/or M2, we hypothesize that uranyl ion formation occurs in parallel to formation of the 3-NBN-derived ligands. From these results, it appears 3-NBN triboluminescence/sublimation during MAI both ionizes the uranyl analytes and generates the M* adduct species simultaneously within the inlet region of the mass spectrometer. Future efforts will explore alternative MAI matrices for uranyl analyte detection and determine if M*-like ligands are unique to 3-NBN. Prior research has also shown 3-NBN primarily generates positive ions[55]. We hypothesize that alternative MAI matrices such as 2-nitrobenzonitrile or 1,2-dicyanobenzene may increase uranyl ion yields because they generate predominantly negative ions when subjected to vacuum. This may lead to potential improvement of LODs to sub nanogram quantities and provide new insights into MAI phenomena.

CONCLUSION

This research demonstrates viable MAI detection and characterization of several uranyl complexes and demonstrates unoptimized detection limits in the nanogram range. Mass spectral measurements show uranyl ions are easily detected as negative ion complexes and that partial uranyl-ligand chemical speciation is preserved during ionization. Optimization of MAI methods for uranyl or other actinide species of interest via injection method and/or alternative mass spectrometer instrumentation will likely result in greatly increased sensitivity and reduce carryover within the instrument. The observed gas-phase speciation is similar to what has been reported for negative ESI analysis of uranyl compounds with notable differences. Adducts hypothesized to originate from the 3-NBN matrix were identified in some uranyl ion complexes which are not characteristic of ESI. On the basis of the limited analysis, these anions are likely matrix-derived, are formed during the ionization process, and are not spurious contaminants of the 3-NBN feedstock. Further examination of this ionization mechanism is needed and will likely result in better understanding of ion formation for all analytes using negative-ion-mode MAI, both inorganic and organic.

ASSOCIATED CONTENT

Supporting Information

Description of AccuTOF instrument operation and parameters, formula used to calculate ppm for uranyl complexes containing matrix anions, description of GC Q-TOF method and analyses, Figures S1–S6, and Tables S1 and S2 (PDF)

AUTHOR INFORMATION

Corresponding Author

* Matthew S. Wellons – Savannah River National Laboratory, Aiken, South Carolina, 29808; Email: matthew.wellons@srnl.doe.gov

Author Contributions

The manuscript was written through contributions of all authors.

Notes

The authors declare no competing financial interest.

ACKNOWLEDGMENT

This article has been authored by Savannah River Nuclear Solutions LLC under Contract No. DE-AC09-08SR22470 with the US Department of Energy. The United States Government retains and the publisher, by accepting this article for publication, acknowledges that the United States Government retains a non-exclusive, paid-up, irrevocable, worldwide license to publish or reproduce the published form of this work, or allow others to do so, for United States Government purposes. Financial support for this work was provided by the SRNL Laboratory Directed Research & Development (LDRD) program through project number LDRD-2018-0004. The authors thank Dr. Michael Bronikowski for preparing the uranium complex solutions investigated in this study, Dr. Chip Cody at JEOL USA for his training and guidance on the AccuTOF, and the LDRD team members Dr. Kaitlin Lawrence, Ashlee Swindle, and Ross Smith.

REFERENCES

1. Becker, J.; Zoriy, M.; Halicz, L.; Teplyakov, N.; Müller, C.; Segal, I.; Pickhardt, C.; Platzner, I., Environmental monitoring of plutonium at ultratrace level in natural water (Sea of Galilee—Israel) by ICP-SFMS and MC-ICP-MS. *Journal of analytical atomic spectrometry* **2004,** *19*(9), 1257-1261.
2. Zheng, J.; Tagami, K.; Watanabe, Y.; Uchida, S.; Aono, T.; Ishii, N.; Yoshida, S.; Kubota, Y.; Fuma, S.; Ihara, S., Isotopic evidence of plutonium release into the environment from the Fukushima DNPP accident. *Scientific reports* **2012,** *2*, 304.
3. Kimura, Y.; Shinohara, N.; Funatake, Y., Development of prototype nuclear forensics library for nuclear materials and radioisotopes in Japan Atomic Energy Agency. *Energy Procedia* **2017,** *131*, 239-245.
4. Mayer, K.; Wallenius, M.; Ray, I., Nuclear forensics—a methodology providing clues on the origin of illicitly trafficked nuclear materials. *Analyst* **2005,** *130*(4), 433-441.

5. Wallenius, M.; Mayer, K., Age determination of plutonium material in nuclear forensics by thermal ionisation mass spectrometry. *Fresenius' journal of analytical chemistry* **2000,** *366* (3), 234-238.

6. Boulyga, S.; Konegger-Kappel, S.; Richter, S.; Sangely, L., Mass spectrometric analysis for nuclear safeguards. *Journal of Analytical Atomic Spectrometry* **2015,** *30* (7), 1469-1489.

7. Donohue, D., Strengthening IAEA safeguards through environmental sampling and analysis. *Journal of Alloys and Compounds* **1998,** *271*, 11-18.

8. Suzuki, D.; Esaka, F.; Miyamoto, Y.; Magara, M., Direct isotope ratio analysis of individual uranium–plutonium mixed particles with various U/Pu ratios by thermal ionization mass spectrometry. *Applied Radiation and Isotopes* **2015,** *96*, 52-56.

9. Spano, T. L.; Simonetti, A.; Balboni, E.; Dorais, C.; Burns, P. C., Trace element and U isotope analysis of uraninite and ore concentrate: applications for nuclear forensic investigations. *Applied geochemistry* **2017,** *84*, 277-285.

10. Donohue, D. L., Strengthened nuclear safeguards. *Anal. Chem.* **2002,** *74* (1), 28A-35A.

11. Boulyga, S. F.; Koepf, A.; Konegger-Kappel, S.; Macsik, Z.; Stadelmann, G., Uranium isotope analysis by MC-ICP-MS in sub-ng sized samples. *Journal of Analytical Atomic Spectrometry* **2016,** *31* (11), 2272-2284.

12. Agnes, G. R.; Horlick, G., Electrospray mass spectrometry as a technique for elemental analysis: preliminary results. *Applied spectroscopy* **1992,** *46* (3), 401-406.

13. Agnes, G. R.; Horlick, G., Electrospray mass spectrometry as a technique for elemental analysis: quantitative aspects. *Applied spectroscopy* **1994,** *48* (6), 649-654.

14. Agnes, G. R.; Horlick, G., Determination of solution ions by electrospray mass spectrometry. *Applied spectroscopy* **1994,** *48* (6), 655-661.

15. Stewart, I. I.; Horlick, G., Electrospray mass spectra of lanthanides. *Analytical Chemistry* **1994,** *66* (22), 3983-3993.

16. Mollah, S.; Pris, A. D.; Johnson, S. K.; Gwizdala, A. B.; Houk, R., Identification of metal cations, metal complexes, and anions by electrospray mass spectrometry in the negative ion mode. *Analytical chemistry* **2000,** *72* (5), 985-991.

17. Li, F.; Byers, M. A.; Houk, R., Tandem mass spectrometry of metal nitrate negative ions produced by electrospray ionization. *Journal of the American Society for Mass Spectrometry* **2003,** *14* (6), 671-679.

18. Dion, H. M.; Ackerman, L. K.; Hill Jr, H. H., Detection of inorganic ions from water by electrospray ionization-ion mobility spectrometry. *Talanta* **2002,** *57* (6), 1161-1171.

19. Van Stipdonk, M.; Anbalagan, V.; Chien, W.; Gresham, G.; Groenewold, G.; Hanna, D., Elucidation of the collision induced dissociation pathways of water and alcohol coordinated complexes containing the uranyl cation. *Journal of the American Society for Mass Spectrometry* **2003,** *14* (11), 1205-1214.

20. Groenewold, G. S.; Cossel, K. C.; Gresham, G. L.; Gianotto, A. K.; Appelhans, A. D.; Olson, J. E.; Van Stipdonk, M. J.; Chien, W., Binding of molecular O2 to di-and triligated [UO2]+. *Journal of the American Chemical Society* **2006,** *128* (9), 3075-3084.

21. Van Stipdonk, M. J.; Chien, W.; Anbalagan, V.; Bulleigh, K.; Hanna, D.; Groenewold, G. S., Gas-phase complexes containing the uranyl ion and acetone. *The Journal of Physical Chemistry A* **2004,** *108* (47), 10448-10457.

22. Pasilis, S.; Somogyi, Á.; Herrmann, K.; Pemberton, J. E., Ions generated from uranyl nitrate solutions by electrospray ionization (ESI) and detected with Fourier transform ion-cyclotron resonance (FT-ICR) mass spectrometry. *Journal of the American Society for Mass Spectrometry* **2006,** *17* (2), 230-240.

23. Tsierkezos, N. G.; Roithova, J.; Schröder, D.; Oncak, M.; Slavicek, P., Can electrospray mass spectrometry quantitatively probe speciation? Hydrolysis of uranyl nitrate studied by gas-phase methods. *Inorganic chemistry* **2009,** *48* (13), 6287-6296.

24. Luo, M.; Hu, B.; Zhang, X.; Peng, D.; Chen, H.; Zhang, L.; Huan, Y., Extractive electrospray ionization mass spectrometry for sensitive detection of uranyl species in natural water samples. *Analytical chemistry* **2010,** *82* (1), 282-289.

25. Rios, D.; Rutkowski, P. X.; Van Stipdonk, M. J.; Gibson, J. K., Gas-phase coordination complexes of dipositive plutonyl, PuO22+: chemical diversity across the actinyl series. *Inorganic Chemistry* **2011,** *50* (11), 4781-4790.

26. Crawford, C. L.; Fugate, G. A.; Cable-Dunlap, P. R.; Wall, N. A.; Siems, W. F.; Hill Jr, H. H., The novel analysis of uranyl compounds by electrospray-ion mobility-mass spectrometry. *International Journal of Mass Spectrometry* **2013,** *333*, 21-26.

27. Perez, E.; Hanley, C.; Koehler, S.; Pestok, J.; Polonsky, N.; Van Stipdonk, M., Gas phase reactions of ions derived from anionic uranyl formate and uranyl acetate complexes. *Journal of The American Society for Mass Spectrometry* **2016,** *27* (12), 1989-1998.

28. Forbes, T. P.; Szakal, C., Considerations for uranium isotope ratio analysis by atmospheric pressure ionization mass spectrometry. *Analyst* **2019,** *144* (1), 317-323.

29. Groenewold, G.; Oomens, J.; De Jong, W. A.; Gresham, G. L.; McIlwain, M.; Van Stipdonk, M. J., Vibrational spectroscopy of anionic nitrate complexes of UO 2 2+ and Eu 3+ isolated in the gas phase. *Physical Chemistry Chemical Physics* **2008,** *10* (8), 1192-1202.

30. Groenewold, G. S.; De Jong, W. A.; Oomens, J.; Van Stipdonk, M. J., Variable denticity in carboxylate binding to the uranyl coordination complexes. *Journal of the American Society for Mass Spectrometry* **2010,** *21* (5), 719-727.

31. Cody, R. B.; Dane, A. J., Paper spray ionization for ambient inorganic analysis. *Rapid Communications in Mass Spectrometry* **2014,** *28* (8), 893-898.

32. Narayanan, R.; Pradeep, T., Probing coordination complexes by carbon nanotube-assisted low-voltage paper spray ionization mass spectrometry. *Analytical chemistry* **2017,** *89* (20), 10696-10701.

33. Coopersmith, K.; Cody, R. B.; Mannion, J. M.; Hewitt, J. T.; Koby, S. B.; Wellons, M. S., Rapid paper spray mass spectrometry characterization of uranium and exemplar molecular species. *Rapid Communications in Mass Spectrometry* **2019,** *33* (22), 1695-1702.

34. Kumar, P.; Jaison, P. G.; Telmore, V. M.; Sadhu, B.; Sundararajan, M., Speciation of uranium-mandelic acid complexes using electrospray ionization mass spectrometry and density functional theory. *Rapid Communications in Mass Spectrometry* **2017,** *31* (6), 561-571.

35. McLain, D. R.; Steeb, J. L.; Smith, N. A., Use of an ion mobility spectrometer for detecting uranium compounds. *Talanta* **2018,** *184*, 227-234.

36. Coopersmith, K.; Cody, R. B.; Mannion, J. M.; Hewitt, J. T.; Koby, S. B.; Wellons, M. S., Rapid paper spray mass spectrometry characterization of uranium and exemplar molecular species. *Rapid Commun. Mass Spectrom.* **2019,** *33* (22), 1695-1702.

37. Li, J.; Inutan, E. D.; Wang, B.; Lietz, C. B.; Green, D. R.; Manly, C. D.; Richards, A. L.; Marshall, D. D.; Lingenfelter, S.; Ren, Y., Matrix assisted ionization: new aromatic and nonaromatic matrix compounds producing multiply charged lipid, peptide, and protein ions in the positive and negative mode observed directly from surfaces. *Journal of the American Society for Mass Spectrometry* **2012,** *23* (10), 1625-1643.

38. Chakrabarty, S.; Pagnotti, V. S.; Inutan, E. D.; Trimpin, S.; McEwen, C. N., A new matrix assisted ionization method for the analysis of volatile and nonvolatile compounds by atmospheric probe mass spectrometry. *Journal of The American Society for Mass Spectrometry* **2013,** *24* (7), 1102-1107.

39. Inutan, E. D.; Trimpin, S., Matrix assisted ionization vacuum (MAIV), a new ionization method for biological materials analysis using mass spectrometry. *Molecular & Cellular Proteomics* **2013,** *12* (3), 792-796.

40. Trimpin, S.; Inutan, E. D., Matrix assisted ionization in vacuum, a sensitive and widely applicable ionization method for mass spectrometry. *Journal of The American Society for Mass Spectrometry* **2013,** *24* (5), 722-732.

41. Trimpin, S.; Inutan, E. D., New ionization method for analysis on atmospheric pressure ionization mass spectrometers requiring only vacuum and matrix assistance. *Analytical chemistry* **2013,** *85* (4), 2005-2009.

42. Woodall, D. W.; Wang, B.; Inutan, E. D.; Narayan, S. B.; Trimpin, S., High-throughput characterization of small and large

molecules using only a matrix and the vacuum of a mass spectrometer. *Analytical chemistry* **2015,** *87* (9), 4667-4674.

43. Chakrabarty, S.; DeLeeuw, J. L.; Woodall, D. W.; Jooss, K.; Narayan, S. B.; Trimpin, S., Reproducibility and quantification of illicit drugs using matrix-assisted ionization (MAI) mass spectrometry. *Analytical chemistry* **2015,** *87* (16), 8301-8306.

44. Trimpin, S.; Thawoos, S.; Foley, C. D.; Woodall, D. W.; Li, J.; Inutan, E. D.; Stemmer, P. M., Rapid high mass resolution mass spectrometry using matrix-assisted ionization. *Methods* **2016,** *104*, 63-68.

45. Hoang, K.; Pophristic, M.; Horan, A. J.; Johnston, M. V.; McEwen, C. N., High sensitivity analysis of nanoliter volumes of volatile and nonvolatile compounds using matrix assisted ionization (MAI) mass spectrometry. *Journal of The American Society for Mass Spectrometry* **2016,** *27* (10), 1590-1596.

46. Cody, R. B., Ambient Profiling of Phenolic Content in Tea Infusions by Matrix-Assisted Ionization in Vacuum. *Journal of The American Society for Mass Spectrometry* **2018,** *29* (8), 1594-1600.

47. Trimpin, S.; Pophristic, M.; Adeniji-Adele, A.; Tomsho, J. W.; McEwen, C. N., Vacuum Matrix-Assisted Ionization Source Offering Simplicity, Sensitivity, and Exceptional Robustness in Mass Spectrometry. *Analytical chemistry* **2018,** *90* (19), 11188-11192.

48. Lee, C.; Inutan, E. D.; Chen, J. L.; Mukeku, M. M.; Weidner, S. M.; Trimpin, S.; Ni, C. K., Toward understanding the ionization mechanism of matrix-assisted ionization using mass spectrometry experiment and theory. *Rapid Communications in Mass Spectrometry* **2019**.

49. Trimpin, S.; Lutomski, C. A.; El-Baba, T. J.; Woodall, D. W.; Foley, C. D.; Manly, C. D.; Wang, B.; Liu, C.-W.; Harless, B. M.; Kumar, R., Magic matrices for ionization in mass spectrometry. *International Journal of Mass Spectrometry* **2015,** *377*, 532-545.

50. Trimpin, S., " Magic" ionization mass spectrometry. *Journal of the American Society for Mass Spectrometry* **2016,** *27* (1), 4-21.

51. Trimpin, S., Novel ionization processes for use in mass spectrometry: 'Squeezing' nonvolatile analyte ions from crystals and droplets. *Rapid Commun. Mass Spectrom.* **2019,** *33* (S3), 96-120.

52. Devereaux, Z. J.; Reynolds, C. A.; Fischer, J. L.; Foley, C. D.; DeLeeuw, J. L.; Wager-Miller, J.; Narayan, S. B.; Mackie, K.; Trimpin, S., Matrix-Assisted Ionization on a Portable Mass Spectrometer: Analysis Directly from Biological and Synthetic Materials. *Anal. Chem. (Washington, DC, U. S.)* **2016,** *88* (22), 10831-10836.

53. Wang, B.; Dearring, C. L.; Wager-Miller, J.; Mackie, K.; Trimpin, S., Drug detection and quantification directly from tissue using novel ionization methods for mass spectrometry. *European Journal of Mass Spectrometry* **2015,** *21* (3), 201-210.

54. Sokalska, M.; Prussakowska, M.; Hoffmann, M.; Gierczyk, B.; Frański, R., Unusual ion UO 4− formed upon collision induced dissociation of [UO 2 (NO 3) 3]−,[UO 2 (ClO 4) 3]−,[UO 2 (CH 3 COO) 3]− ions. *Journal of the American Society for Mass Spectrometry* **2010,** *21* (10), 1789-1794.

55. Banstola, B.; Murray, K. K., Sublimation Electrification of Organic Compounds. *Journal of the American Society for Mass Spectrometry* **2020,** *31* (4), 888-893.

Matrix Assisted Ionization of Molecular Uranium Species

Danielle R. Mannion, Joseph M. Mannion, Wendy W. Kuhne, Matthew S. Wellons*

Savannah River National Laboratory, Aiken, South Carolina 29803

*Corresponding Author: Matthew S. Wellons, Email: matthew.wellons@srnl.doe.gov

Supporting Information

AccuTOF Instrument Operation and Parameters

To facilitate access to the atmospheric pressure sampling orifice, the DART ion source was placed in stand-by and retracted on its rail. Mass spectra were acquired in negative ion mode at a resolving power of 10,000 (FWHM). The RF ion guide was set to 800 V to pass ions greater than approximately 80 *m/z* and spectra were acquired for the mass-to-charge range corresponding to 100 – 1500 *m/z*. The atmospheric pressure interface potentials were set to the following values: orifice 1 = -50 V, ring lens and orifice 2 = -5 V, and the detector voltage was set to -2700 V. The atmospheric pressure orifice temperature was set to 150 °C to limit the ionization duration of each sample to approximately 5 seconds for higher through-put. At the end of an analysis series, the DART source was turned on and moved to 14 mm from orifice 1 to perform the Fomblin Y calibration.

Formula to Calculate ppm of Ion Complexes Containing Unknown Matrix Adducts:

$$\frac{(UO_2 + \text{Anion(s)} + M^*) - (\text{Ion Complex})}{(UO_2 + \text{Anion(s)} + M^*)} \times 10^6$$

UO_2 = exact mass of uranyl

Anions(s) = exact mass of putative anion conjugates

M* = measured mass of matrix-derived ions

Ion Complex = measured mass of the uranyl ion complex

GC Q-TOF Method and Analyses

An Agilent 7250 GC/Q-TOF mass spectrometer was used to characterize the 3-NBN matrix for potential impurities. The instrument was equipped with an Agilent HP-5MS 5% Phenyl Methyl Siloxane 30 m x 250 µm x 0.25 µm column. An Agilent Ultra Inert splitless double taper inlet liner was used with a setpoint temperature of 250 °C. The oven initial temperature was 45 °C with a 2.25 min hold and a 20 °C/min ramp to 280 °C with a 5 min solvent hold. 3-NBN samples were diluted to 1 ng/µL in methanol with 1 µL injection volumes. An electron energy of 70 eV was used. EICs shown in Figure S3 were extracted from the TIC using a ± 10 ppm error based on the experimental masses determined utilizing the AccuTOF MS for unknown species corresponding with M* m/z. No ion signals consistent with M* species were observed. Ion signals are present as weaker peaks within the EIC but are consistent with spurious background interferents. All ion peaks present in the M1-6 chromatograms correlate with regions of high mass error (>5 ppm). Broader EIC extraction windows are shown in Figure S3 to demonstrate that M1-M6 species were not overlooked due to mass calibration differences between the Q-TOF and AccuTOF MS. Low energy EI (~5 eV) was also explored due to the possibility of high molecular ion fragmentation; similar results were obtained utilizing low electron energies.

Supporting Figures

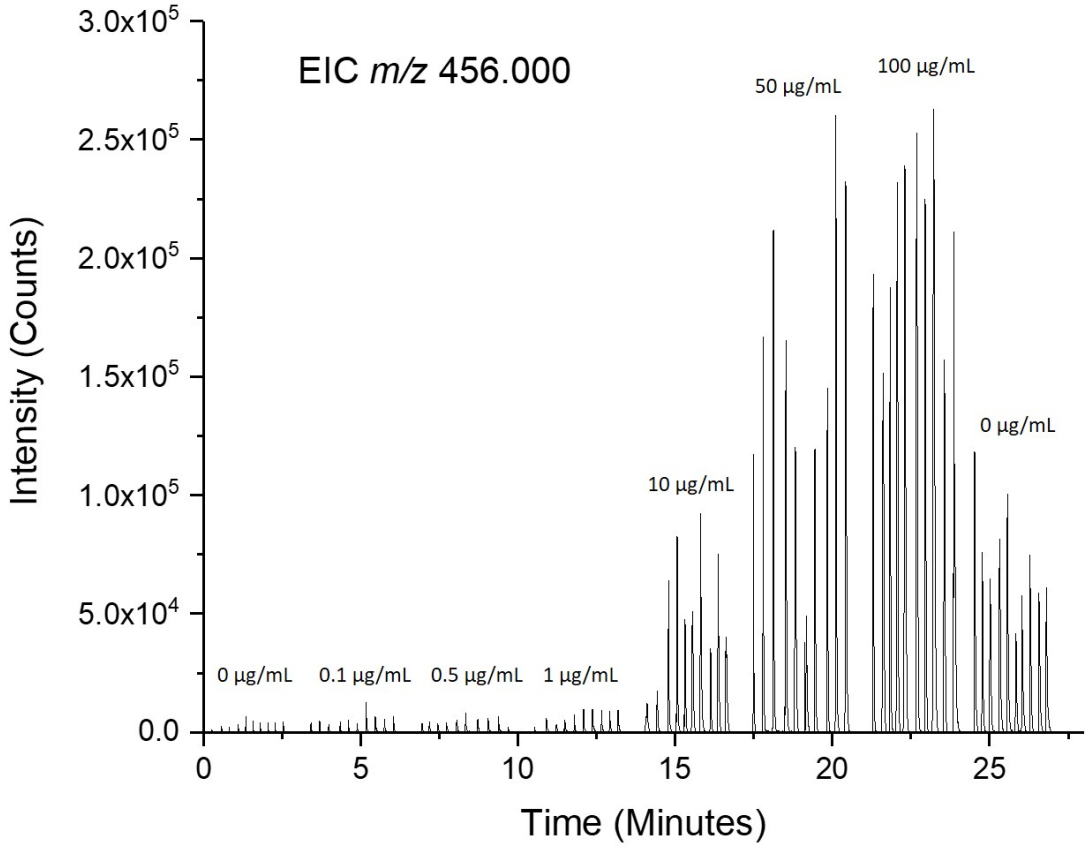

Figure S1. The Extracted Ion Chromatogram (EIC) of the highest intensity analyte ion observed for the analysis of uranyl nitrate in negative ion mode by Matrix Assisted Ionization (MAI). Solutions were analyzed in increasing concentration with 10 aspirations performed per solution.

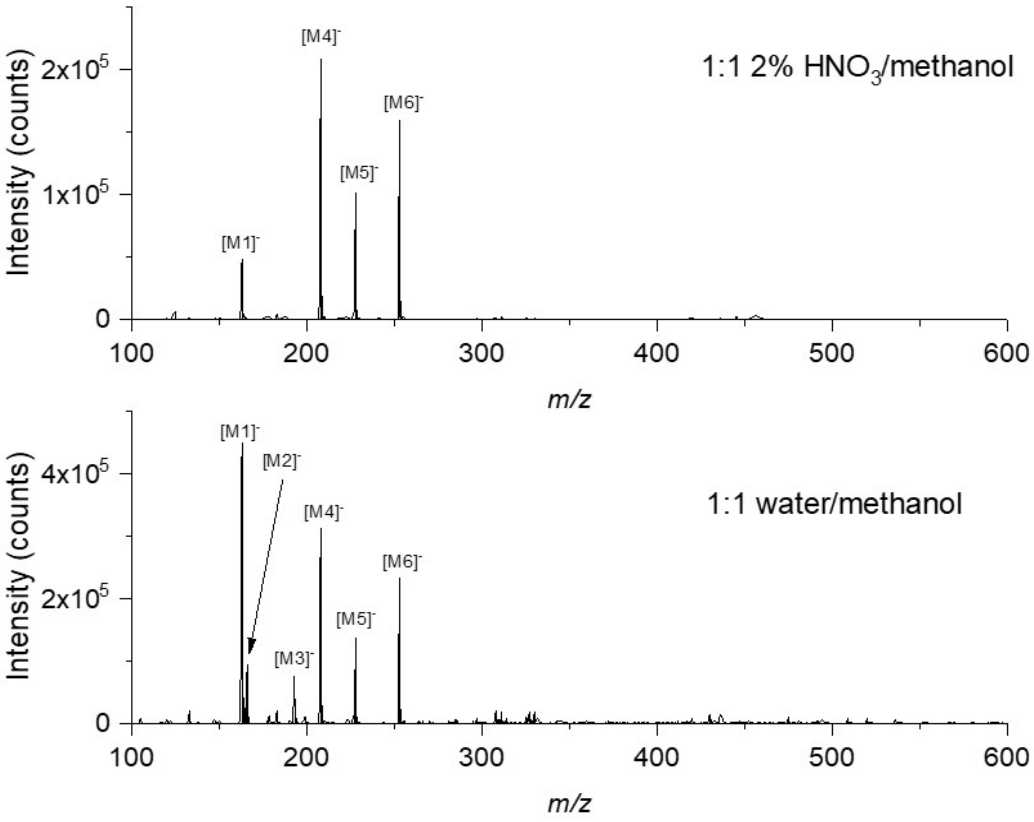

Figure S2. Spectra of the matrix ions observed when analyzing 3-NBN in 1:1 2% nitric acid/methanol (top) and 1:1 water/methanol (bottom).

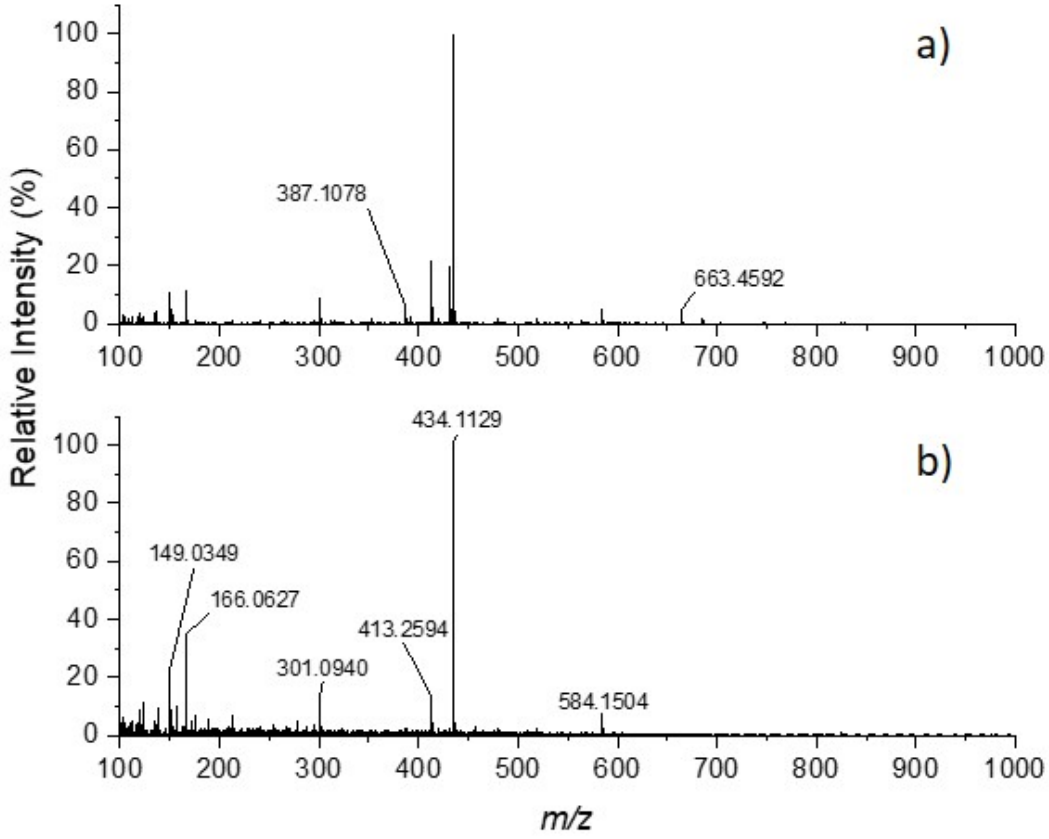

Figure S3. MAI spectra collected in positive ion mode of 100 µg/mL $UO_2(NO_3)_2$ (a) and 3-NBN in 1:1 water/methanol (b). Two low intensity peaks that are uniquely observed in the uranyl nitrate spectra are labeled.

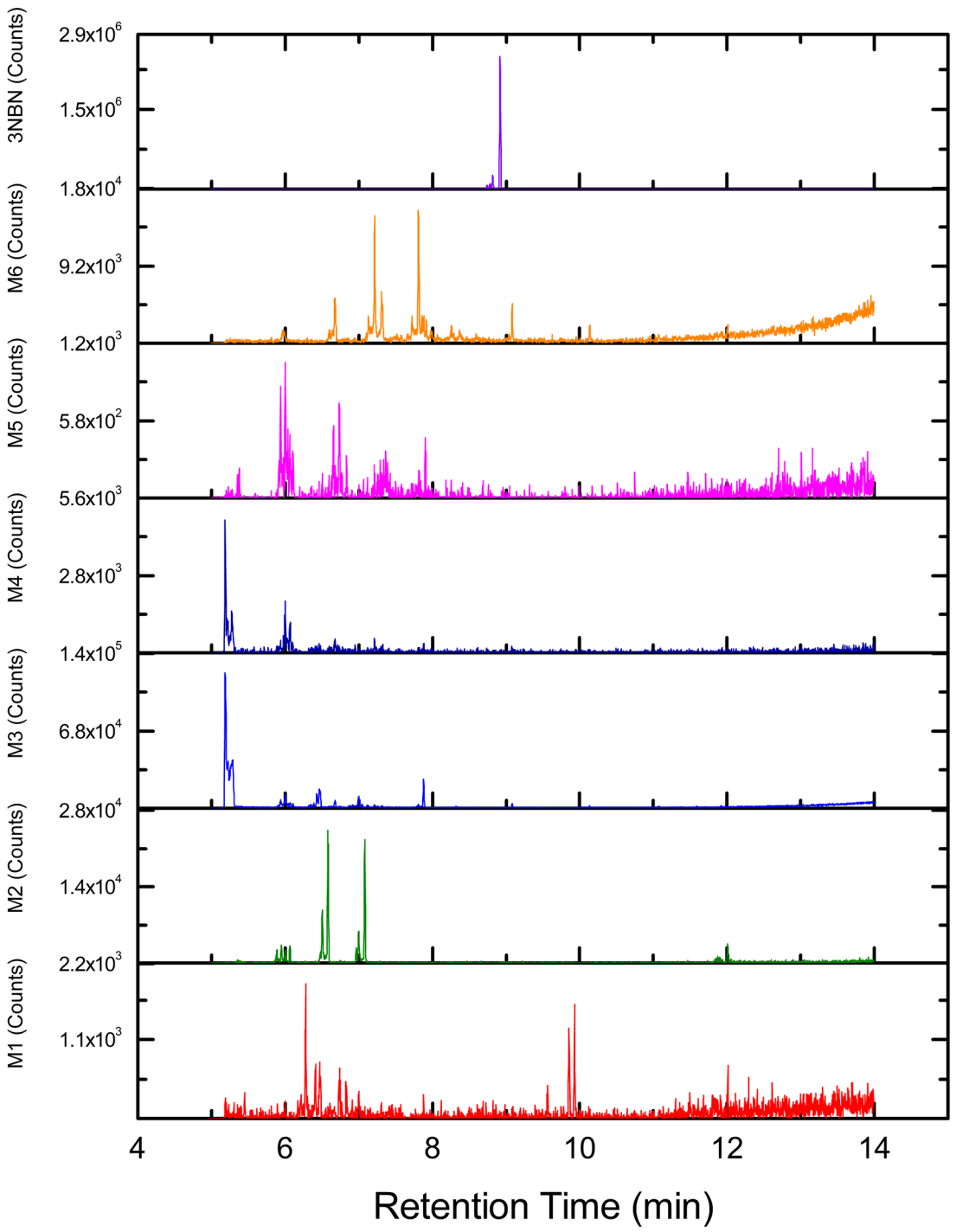

Figure S4. EIC measurements from an Agilent 7250 GC/Q-TOF with identification of 3-NBN (top) and regions of the m/z regime expected for the M* species observed from MAI experiments on the JEOL AccuTOF. No significant intensities consistent with M* species were observed.

Table S1. Complete list of uranyl analyte ions identified above 10% relative ion intensity threshold.

Proposed Identity	Calculated Mass	Measured Mass	ppm	Relative Intensity %
Uranyl Nitrate ($UO_2(NO_3)_3$ in 2% HNO_3)				
$UO_2(NO_3)_3^-$	456.0041	456.0005	7.85	100.00%
$UO_2(NO_3)_2$ (M2)$^-$	560.0265	560.0247	3.17	23.27%
$UO_2(NO_3)_2$ O$^-$	410.0112	410.0063	11.8	19.36%
$UO_2(NO_3)$ $(OH)_2^-$	366.0339	366.0289	13.8	11.57%
Uranyl Chloride (UO_2Cl_2 in water)				
UO_2Cl (M1) (M2)$^-$	634.0300	634.0321	3.35	70.25%
UO_2 $(M2)_2$ (M1)$^-$	765.0714	765.0753	5.09	67.88%
UO_2Cl_2 (M2)$^-$	505.9886	505.9865	4.17	38.21%
UO_2 (M2) $(M1)_2^-$	762.0714	762.0753	5.07	37.55%
UO_2 $(M2)_3^-$	768.0713	768.0750	4.79	35.54%
UO_2Cl $(M2)_2^-$	637.0299	637.0306	1.08	33.85%
$UO_2Cl_3^-$	374.9472	374.9423	13.1	31.36%
UO_2Cl_2 (M1)$^-$	502.9886	502.9907	4.23	17.63%
Uranyl Acetate ($UO_2(CH_3CO_2)_2$ in water)				
$UO_2(CH_3CO_2)_3^-$	447.0805	447.0805	0.04	100.00%
$UO_2(CH_3CO_2)_2O_2^-$	420.0571	420.0546	5.76	39.41%
$UO_2(CH_3CO_2)_2$(M2)$^-$	554.0775	554.0792	3.06	24.77%
UO_2 $(M2)_2$(M1)$^-$	765.0714	765.0790	10.0	21.56%
UO_2 (M2) $(M1)_2^-$	762.0714	762.0795	10.7	19.41%
$UO_2(CH_3CO_2)$ (M1) (M2)$^-$	658.0744	658.0786	6.26	11.26%
$UO_2(CH_3CO_2)_2$(M1)$^-$	551.0775	551.0784	1.59	11.20%
$UO_2(CH_3CO_2)$ $(M2)_2^-$	661.0744	661.0803	8.86	10.97%
$UO_2(CH_3CO_2)_2OH^-$	405.0700	405.0672	6.89	10.87%
Uranyl Oxalate ($UO_2C_2O_4$ in water)				
$UO_2(C_2O_4)$ (M2)$^-$	524.0305	524.0314	1.63	42.98%
UO_2 $(OH)_2$ (M2)$^-$	470.0563	470.0571	1.63	26.76%
$UO_2(C_2O_4)$ OH^-	375.0230	375.0209	5.52	24.32%
UO_2 $(OH)_3^-$	321.0488	321.0452	11.4	23.87%
$UO_2(C_2O_4)$ $HC_2O_4^-$	447.0078	447.0057	4.63	17.82%
$UO_2(C_2O_4)$ CO_2^-	402.0101	402.0082	4.85	16.25%
UO_2 O_2^-	302.0304	302.0278	8.84	15.98%

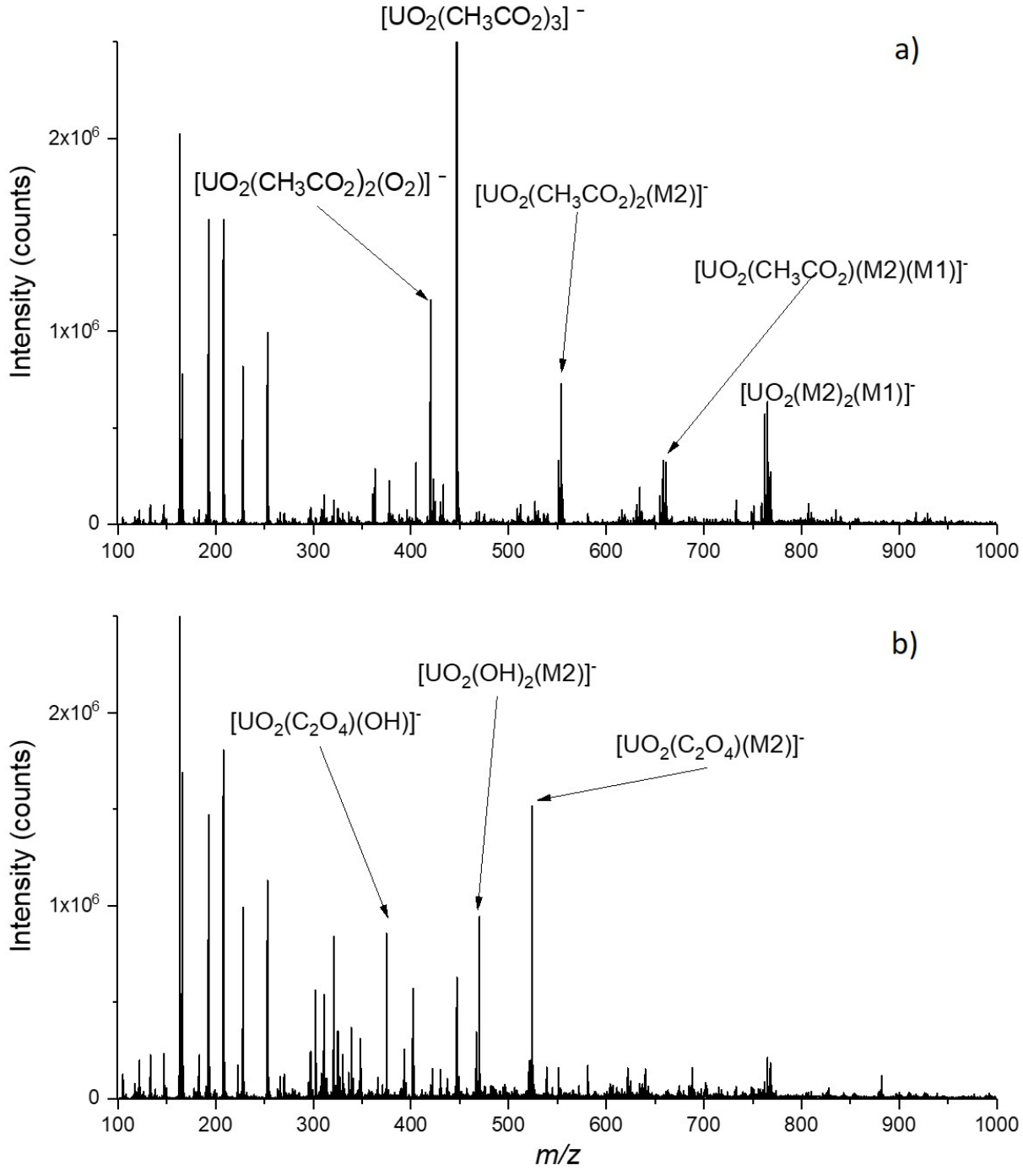

Figure S5. Negative ion mode mass spectra collected for uranyl acetate (a) and uranyl oxalate (b) using MAI. Predominant ion complexes are labeled with putative identities. Peaks below 275 m/z are matrix-derived anions described within the publication text.

Table S2. The measured mass of matrix-derived anions below 275 m/z.

ID	Measured m/z
M1	163.01027
M2	166.01024
M3	193.02147
M4	207.99582
M5	227.98590
M6	252.98073

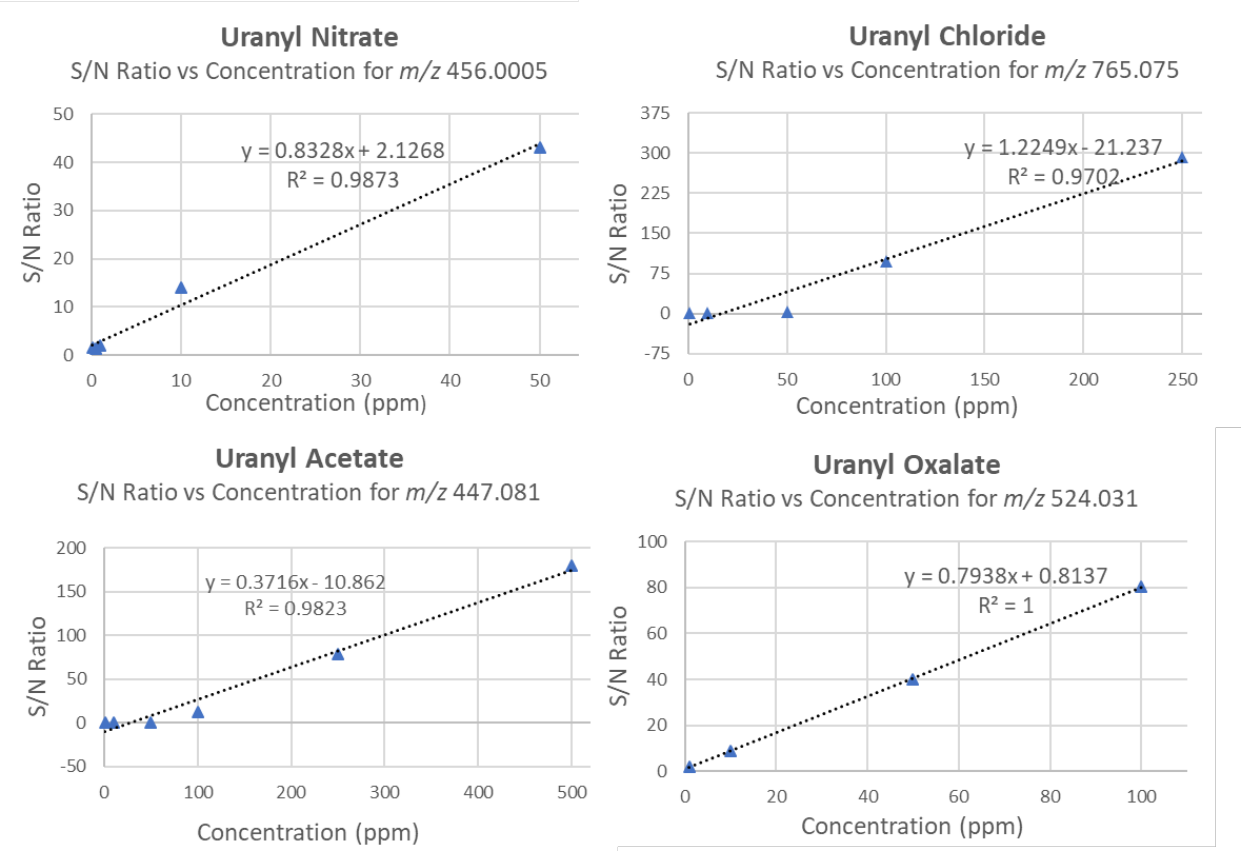

Figure S6. Linear regression plots of uranyl nitrate, chloride, acetate, and oxalate used to calculate the Limit of Detection (LOD) for each uranyl-ligand species.